MABS
2017, VOL. 9, NO. 1, 154–164
http://dx.doi.org/10.1080/19420862.2016.1255389

Taylor & Francis
Taylor & Francis Group

REPORT

Development and preclinical studies of ^{64}Cu-NOTA-pertuzumab F(ab′)$_2$ for imaging changes in tumor HER2 expression associated with response to trastuzumab by PET/CT

Karen Lam[a], Conrad Chan[a], and Raymond M. Reilly[a,b,c]

[a]Department of Pharmaceutical Sciences, University of Toronto, Toronto, ON, Canada; [b]Department of Medical Imaging, University of Toronto, Toronto, ON, Canada; [c]Toronto General Research Institute, University Health Network, Toronto, ON, Canada

ABSTRACT

We previously reported that microSPECT/CT imaging with ^{111}In-labeled pertuzumab detected decreased HER2 expression in human breast cancer (BC) xenografts in athymic mice associated with response to treatment with trastuzumab (Herceptin). Our aim was to extend these results to PET/CT by constructing F(ab′)$_2$ of pertuzumab modified with NOTA chelators for complexing ^{64}Cu. The effect of the administered mass (5–200 μg) of ^{64}Cu-NOTA-pertuzumab F(ab′)$_2$ was studied in NOD/SCID mice engrafted with HER2-positive SK-OV-3 human ovarian cancer xenografts. Biodistribution studies were performed in non-tumor bearing Balb/c mice to predict radiation doses to normal organs in humans. Serial PET/CT imaging was conducted on mice engrafted with HER2-positive and trastuzumab-sensitive BT-474 or trastuzumab-insensitive SK-OV-3 xenografted mice treated with weekly doses of trastuzumab. There were no significant effects of the administered mass of ^{64}Cu-NOTA-pertuzumab F(ab′)$_2$ on tumor or normal tissue uptake. The predicted total body dose in humans was 0.015 mSv/MBq, a 3.3-fold reduction compared to ^{111}In-labeled pertuzumab. MicroPET/CT images revealed specific tumor uptake of ^{64}Cu-NOTA-pertuzumab F(ab′)$_2$ at 24 or 48 h post-injection in mice with SK-OV-3 tumors. Image analysis of mice treated with trastuzumab showed 2-fold reduced uptake of ^{64}Cu-NOTA-pertuzumab F(ab′)$_2$ in BT-474 tumors after 1 week of trastuzumab normalized to baseline, and 1.9-fold increased uptake in SK-OV-3 tumors after 3 weeks of trastuzumab, consistent with tumor response and resistance, respectively. We conclude that PET/CT imaging with ^{64}Cu-NOTA-pertuzumab F(ab′)$_2$ detected changes in HER2 expression in response to trastuzumab while delivering a lower total body radiation dose compared to ^{111}In-labeled pertuzumab.

ARTICLE HISTORY
Received 28 June 2016
Revised 22 October 2016
Accepted 26 October 2016

KEYWORDS
Copper-64; HER2; molecular imaging; pertuzumab; PET; radiation dosimetry; trastuzumab

Introduction

The human epidermal growth factor receptor-2 (HER2) is over-expressed in 15–20% of breast cancers (BC) and confers a poor prognosis.[1-3] Treatment with trastuzumab (Herceptin, Roche), a humanized IgG$_1$ anti-HER2 monoclonal antibody (mAb) combined with chemotherapy improves patient outcome in the adjuvant and metastatic settings in patients who have BC that is defined as HER2-positive either by immunohistochemistry (IHC) or *in situ* hybridization (ISH) analyses.[4-6] Guidelines have been established to define tumor HER2 positivity using these techniques.[7] Despite the establishment of trastuzumab as the standard-of-care for treatment of HER2-positive BC, clinical trials revealed that only 1 in 2 patients with HER2-positive tumors responded to trastuzumab combined with chemotherapy[4] and most responding patients acquire resistance within a year.[8] It has also been proposed that some patients with BC classified as HER2-negative may also receive benefit from trastuzumab.[9]

Molecular imaging which includes single photon emission computed tomography (SPECT) and positron emission tomography (PET) provides a sensitive tool to non-invasively assess tumor phenotype at any location in the body and monitor response to targeted cancer therapies.[10] One proposed mechanism of action of trastuzumab involves the induction of HER2 internalization, which reduces the density of HER2 on tumor cells available for receptor dimerization and oncogenic signaling.[11] Probing changes in HER2 expression in tumors could be a promising strategy to discriminate responders from non-responders to trastuzumab treatment. Pertuzumab is a humanized IgG$_1$ mAb that binds domain II on HER2 and hinders receptor dimerization.[12] Because the HER2 binding domain of pertuzumab is distinct from that of trastuzumab (domain IV) and pertuzumab has a different mechanism of action than trastuzumab,[13] these mAbs have been administered in combination to improve patient outcome.[14,15] We previously reported that microSPECT/CT imaging with ^{111}In-labeled pertuzumab sensitively detected changes in HER2 expression in MDA-MB-361 human BC xenografts in athymic mice following treatment with trastuzumab, based on our finding that the binding of the imaging probe to HER2 is not affected by trastuzumab binding.[16] Decreased HER2 expression was detected by imaging as early as 3 days after commencing trastuzumab treatment, and images at 21 days demonstrated significantly lower tumor uptake of ^{111}In-labeled pertuzumab was associated with almost complete tumor eradication. Our group has launched a Phase 1/2 clinical trial (PETRA trial; ClinicalTrials.gov identifier

CONTACT Raymond M. Reilly raymond.reilly@utoronto.ca Pharmaceutical Sciences, University of Toronto, Leslie Dan Faculty of Pharmacy, 144 College St., Toronto, ON, Canada, M5S 3M2.

NCT01805908) investigating SPECT/CT imaging with ^{111}In-labeled pertuzumab to detect changes in tumor HER2 expression in patients with metastatic BC treated with trastuzumab and chemotherapy. The clinical formulation and translational preclinical studies that were required to advance this imaging agent to clinical trial are reported elsewhere.[17,18]

In the study reported here, our aim was to develop an analogous positron-emitting imaging probe based on pertuzumab to detect trastuzumab-mediated HER2 internalization that would extend these promising findings to PET, and potentially reduce the radiation dose associated with the 3 administrations of ^{111}In-labeled pertuzumab required in the PETRA clinical trial protocol. The predicted combined total body radiation dose for these 3 imaging studies performed at baseline, 1 week and 4 weeks after commencing treatment with trastuzumab and chemotherapy was 17 mSv, based on an administered amount of 111 MBq of ^{111}In-labeled pertuzumab for each study (0.05 mSv/MBq).[18] PET is 100-fold more sensitive than SPECT and yields high resolution images that are more accurately quantitated.[19] ^{64}Cu is an attractive positron-emitter for labeling pertuzumab because it is produced in a biomedical cyclotron,[20] emits a moderate energy positron [0.7 MeV (19%)] that provides good intrinsic spatial resolution (0.7 mm), and is strongly complexed by macrocyclic chelators such as 1,4,7-triazacyclononane-1,4,7-triacetate (NOTA) that are easily conjugated to antibodies.[21] Due to the short half-life of ^{64}Cu ($t_{1/2}$ = 12.7 h), it is necessary to employ mAb fragments [e.g., Fab or F(ab′)$_2$], which are taken up by tumors but rapidly eliminated from the blood and most normal tissues, to provide high tumor:blood ratios within the useful lifetime of the radionuclide [up to 48 h post-injection (p.i)]. The short half-life of ^{64}Cu combined with the rapid elimination of mAb fragments is expected to minimize the radiation dose for the imaging procedure. We report here the synthesis and characterization of ^{64}Cu-NOTA-pertuzumab F(ab′)$_2$ and its first evaluation for detecting changes in HER2 expression and response to treatment in athymic mice with trastuzumab-sensitive BT-474 human BC xenografts and trastuzumab-resistant SK-OV-3 human ovarian cancer xenografts. We further studied the effect of increasing the administered mass of ^{64}Cu-NOTA-pertuzumab F(ab′)$_2$ on tumor and normal tissue uptake, and projected the radiation absorbed doses in humans based on its pharmacokinetics of uptake and elimination from normal organs in mice.

Results

^{64}Cu-NOTA-pertuzumab F(ab′)$_2$

F(ab′)$_2$ were obtained in high purity (>90%) by pepsin digestion of pertuzumab IgG as shown by SE-HPLC analysis, which demonstrated a single peak (not shown), and by SDS-PAGE analysis (Fig. 1A), which revealed one major band associated with a protein with $M_r \approx 110$ kDa. The chelate substitution level achieved for F(ab′)$_2$ concentrations of 2.5, 5, or 10 mg/mL reacted with a 5- or 10-fold molar excess of p-SCN-Bn-NOTA are shown in Table 1. NOTA-pertuzumab F(ab′)$_2$ exhibited a single major band on SDS-PAGE analysis (Fig. 1B). The substitution levels of NOTA per pertuzumab F(ab′)$_2$ measured from the ITLC-SG assay were in good agreement with those measured by the UV spectrophotometric assay (Table 1). The reaction using 2.5 mg/mL of F(ab′)$_2$ protein and a 10-fold molar excess of NOTA yielded a substitution level of 4.1 ± 1.9 NOTA/F(ab′)$_2$, and these reaction conditions were used for all subsequent experiments. Following purification by ultrafiltration, the final radiochemical purity of ^{64}Cu-NOTA-pertuzumab F(ab′)$_2$ was 85–95% by both ITLC-SG and SE-HPLC (Fig. 1C). ^{64}Cu-NOTA-F(ab′)$_2$ demonstrated saturable binding to SK-

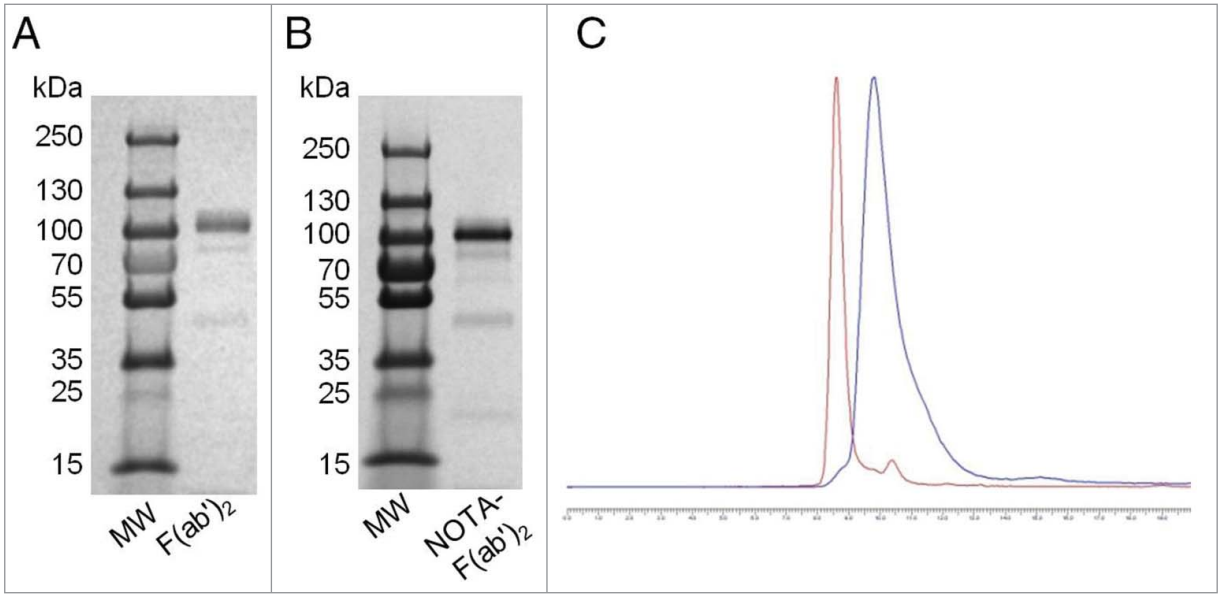

Figure 1. SDS-PAGE analysis of unconjugated F(ab′)$_2$ (A) and NOTA-F(ab′)$_2$ immunoconjugate (B). A protein ladder for standard molecular weights (MW) is also shown. (C) SE-HPLC analysis with ultraviolet (UV) detection at 280 nm of ^{64}Cu-NOTA-pertuzumab F(ab′)$_2$ [retention time (t_R) = 8.5 mins; red line] and the corresponding chromatogram obtained by radioactivity detection using a flow scintillation analyzer (FSA) detector (t_R = 9.8 mins; blue line). The small peak on the UV trace with t_R = 10.4 mins represents low molecular weight impurities including unconjugated NOTA (<5%). The offset for the radiochromatogram relative to UV detection corresponds to the time interval required for eluate to flow from the UV to FSA detector which are in sequence. The larger flow cell of the FSA detector causes peak broadening compared to the UV detector. The chemical and radiochemical purity of ^{64}Cu-NOTA-pertuzumab F(ab′)$_2$ by SE-HPLC analysis was >95%.

Table 1. Chelate:protein substitution levels under different reaction conditions for NOTA conjugation of pertuzumab F(ab′)$_2$.

	F(ab′)$_2$ protein concentration (mg/mL)					
	2.5		5.0		10.0	
Molar ratio of NOTA:F(ab′)$_2$	ITLC-SG*	UV assay†	ITLC-SG	UV assay	ITLC-SG	UV assay
5:1	2.1 ± 0.0	2.8 ± 1.1	3.8 ± 0.4	3.7 ± 1.7	4.3 ± 2.5	5.8 ± 2.9
10:1	4.1 ± 1.9	4.2 ± 1.4	6.9 ± 1.8	5.0 ± 1.1	6.5 ± 1.8	9.9 ± 8.8

Values shown are mean ± SD (n = 3–8).
*Instant thin layer-silica gel chromatography developed in 0.1 M sodium citrate, pH 5.0.
†Measurement of absorbance at 280 nm with subtraction of the contribution from pertuzumab F(ab′)$_2$.

BR-3 cells with K_d and B_{max} values of 2.6 ± 0.3 nM and 0.9 ± 0.3 × 10^6 receptors/cell, respectively. These values were similar to those reported by our group for ^{111}In-BzDTPA-pertuzumab (K_d = 2.0–5.3 nM, B_{max} = 1.2–1.3 ×10^6 receptors/cell).[16,17]

Trastuzumab-mediated HER2 internalization

The binding of ^{64}Cu-NOTA-pertuzumab F(ab′)$_2$ by BT-474 cells was significantly reduced to 67.0 ± 8.1% ($P < 0.05$) following exposure to trastuzumab (14 μg/mL) at 37°C for 24 h compared to untreated cells, which was set at 100%. Trastuzumab exposure significantly reduced the binding of ^{64}Cu-NOTA-pertuzumab F(ab′)$_2$ to SK-OV-3 cells to 85.5 ± 3.8% compared to untreated cells ($P < 0.05$). Thus, comparing trastuzumab-sensitive BT-474 cells with trastuzumab-resistant SK-OV-3 cells, trastuzumab was 2.2-fold more effective at decreasing the binding of ^{64}Cu-NOTA-pertuzumab F(ab′)$_2$ to BT-474 than SK-OV-3 cells ($P < 0.05$).

Biodistribution, pharmacokinetic and radiation dosimetry studies

The tumor and normal tissue uptake of increasing mass amounts of ^{64}Cu-NOTA-pertuzumab F(ab′)$_2$ (5, 50, 100 or 200 μg) at 24 h post-injection (p.i.) in NOD/SCID mice bearing HER2-overexpressing SK-OV-3 tumor xenografts are shown in Table 2. The greatest uptake for all amounts was observed in the kidneys (52.4–65.6 %ID/g), followed by the spleen (7.4–11.9 %ID/g) and liver (7.8–10.9 %ID/g), but no statistically significant differences were observed between groups receiving different masses of ^{64}Cu-NOTA-pertuzumab F(ab′)$_2$ (P = 0.357, 0.173 and 0.191, respectively). There appeared to be slightly lower tumor uptake for the 200 μg administered amount (5.8 ± 1.3 %ID/g) compared to 5 μg (8.2 ± 2.6 %ID/g), 50 μg (9.8 ± 5.1 %ID/g or 100 μg (8.2 ± 2.1 %ID/g), but these differences were not significant (P = 0.210). Tumor/blood (T/B) ratios for 5, 50, 100 or 200 μg amounts of ^{64}Cu-NOTA-pertuzumab F(ab′)$_2$ were 14.4 ± 5.14, 18.6 ± 7.4, 15.7 ± 0.8, and 11.2 ± 1.9, respectively. Tumor/muscle (T/M) ratios for 5, 50, 100 or 200 μg amounts of ^{64}Cu-NOTA-pertuzumab F(ab′)$_2$ were 22.4 ± 6.6, 25.1 ± 12.7, 23.7 ± 5.6, and 15.6 ± 5.7, respectively. There were no significant differences in T/B (P = 0.205) or T/M ratios (P = 0.405) for different masses of ^{64}Cu-NOTA-pertuzumab F(ab′)$_2$. An administered amount of 50 μg was selected for subsequent imaging and biodistribution studies.

The elimination of radioactivity from the blood of non-tumor bearing Balb/c mice following intravenous (i.v.; tail vein) injection of ^{64}Cu-NOTA-pertuzumab F(ab′)$_2$ was fitted to a 2-compartment model (Fig. 2). The distribution half-life ($t_{1/2}\alpha$) was 1.3 h and the elimination half-life ($t_{1/2}\beta$) was 10.4 h. The volume of distribution of the central compartment (V_1) was 4.0 mL, the volume of distribution at steady-state (V_{ss}) was 9.6 mL, and the systemic clearance was 1.6 mL/h. Biodistribution studies (Table 3) showed some differences in normal tissue uptake between non-tumor-bearing Balb/c mice and tumor-bearing NOD/SCID mice (Table 2) at 24 h p.i. of ^{64}Cu-NOTA-pertuzumab F(ab′)$_2$ (50 μg), particularly for the liver and

Table 2. Tumor and normal tissue distribution at 24 h post-injection of increasing mass amounts of ^{64}Cu-NOTA-pertuzumab F(ab′)$_2$ *in mice with subcutaneous SK-OV-3 human ovarian cancer xenografts.

	Percent injected dose/g (%ID/g)			
Tissue	5 μg	50 μg	100 μg	200 μg
Blood	0.6 ± 0.0	0.5 ± 0.2	0.5 ± 0.2	0.5 ± 0.1
Heart	2.3 ± 0.3	2.2 ± 0.4	2.0 ± 0.2	1.9 ± 0.3
Lungs	2.1 ± 0.2	2.1 ± 0.4	1.9 ± 0.2	2.0 ± 0.3
Liver	10.7 ± 1.3	10.9 ± 3.3	9.3 ± 2.1	7.8 ± 1.3
Kidneys	60.0 ± 4.7	65.6 ± 16. 2	54.8 ± 3.9	52.4 ± 12.8
Spleen	11.9 ± 0.9	11.5 ± 5.8	9.0 ± 1.4	7.4 ± 0.4
Stomach	2.8 ± 2.9	1.2 ± 0.2	1.1 ± 0.1	1.1 ± 0.1
Intestines	2.1 ± 0.1	2.0 ± 0.4	1.7 ± 0.2	1.8 ± 0.4
Muscle	0.4 ± 0.0	0.4 ± 0.2	0.4 ± 0.1	0.4 ± 0.1
Bone	1.9 ± 0.2	1.6 ± 0.5	1.6 ± 0.2	1.4 ± 0.2
Skin	1.0 ±0.4	1.0 ± 0.6	1.5 ± 1.0	1.5 ± 0.8
Tumor	8.2 ± 2.6	9.8 ± 5.1	8.2 ± 2.1	5.8 ± 1.3

Values shown are mean ± SD (n = 4).
*Mice were intravenously administered 1-3 MBq of ^{64}Cu-NOTA-pertuzumab F(ab′)$_2$.

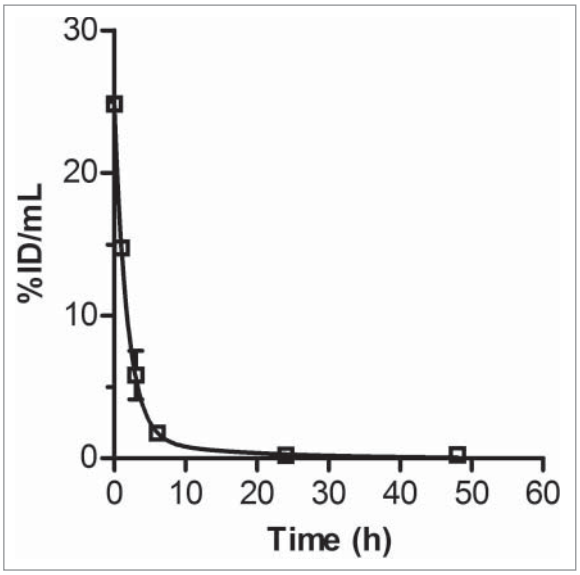

Figure 2. Radioactivity vs. time curve for the elimination of ^{64}Cu-NOTA-F(ab′)$_2$ from the blood of non-tumor-bearing Balb/c mice after intravenous (tail vein) injection. The curve was fitted to a 2-compartment model with i.v. bolus input using Scientist Ver. 2.01 software (MicroMath).

spleen, which were approximately 2-fold and 3-fold lower, respectively, in Balb/c mice. The greatest accumulation of radioactivity was found in the kidneys with lower uptake in the liver and spleen, with the maximum uptake at 3 h p.i. (81.0 ± 21.3, 8.4 ± 2.3 and 7.4 ± 2.4 %ID/g, respectively), decreasing by 2-fold at 48 h p.i. (45.0 ± 4.0, 4.7 ± 0.5, 3.2 ± 0.5 %ID/g; Table 3). The uptake and elimination of radioactivity from normal tissues in mice after i.v. injection of ^{64}Cu-NOTA-pertuzumab F(ab′)$_2$ was used to project the radiation absorbed doses in human female adults. These estimates revealed that the kidneys would receive the highest radiation dose (1 mSv/MBq), followed by the lower large intestine, and liver (Table 4). The estimated whole body equivalent dose was 0.015 mSv/MBq.

MicroPET/CT imaging studies

Representative microPET/CT images of ^{64}Cu-NOTA-pertuzumab F(ab′)$_2$ in mice bearing SK-OV-3 tumors at 24 h p.i. (Fig. 3A) and 48 h p.i. (Fig. 3B) showed accumulation in the tumor but low normal organ uptake with the exception of the kidneys. Images were comparable between the 2 time points. Tumor uptake was visibly diminished in mice that received excess unlabeled pertuzumab 24 h prior to ^{64}Cu-NOTA-pertuzumab F(ab′)$_2$ (Fig. 3C) or that were injected with non-specific ^{64}Cu-NOTA-hIgG F(ab′)$_2$ (Fig. 3D). Biodistribution studies at 48 h (Fig. 3E) revealed a significant 2.2- or 3.1-fold lower tumor uptake for mice receiving excess pertuzumab or injected with ^{64}Cu-NOTA-hIgG F(ab′)$_2$ compared to mice injected with ^{64}Cu-NOTA-pertuzumab F(ab′)$_2$ (3.9 ± 1.0 and 2.7 ± 0.5 %ID/g vs. 8.4 ± 3.4, respectively $P < 0.05$). These results demonstrated that ^{64}Cu-NOTA-pertuzumab F(ab′)$_2$ accumulated specifically in HER2-positive SK-OV-3 tumor xenografts.

MicroPET/CT images of mice bearing BT-474 human BC xenografts revealed diminished uptake of ^{64}Cu-NOTA-F(ab′)$_2$ at 5 days after administration of a loading dose of trastuzumab (4 mg/kg) compared to baseline images (Fig. 4A). VOI analyses revealed highly variable tumor uptake between mice but the mean tumor uptake at baseline and at 1 week after trastuzumab treatment were 6.8 ± 4.4 and 5.1 ± 4.9 %ID/g, respectively. To control for the variability between mice, the %ID/g values at 1 week were divided by the baseline value for each mouse, in order to calculate a normalized ratio of %ID/g. There was a significant decrease in the normalized %ID/g ratio for BT-474 tumors compared to baseline (0.4 ± 0.3, $P < 0.05$, Fig. 4B). Tumor size, measured with calipers, decreased following trastuzumab treatment and mirrored the VOI analysis results (TGI = 0.6 ± 0.2, $P < 0.05$, Fig. 4C). It was not possible to determine changes in tumor volume at week 3 in mice with BT-474 tumors, because only 4 mice were available for measurement of tumor dimensions and these mice exhibited complete response to trastuzumab which precluded tumor measurement. Images of mice bearing SK-OV-3 tumors and treated with trastuzumab (4 mg/kg loading dose then 2 mg/mg weekly for 2 weeks) showed an apparent increase in radiotracer uptake at week 1 and 3 (Fig. 4D). Tumor uptake values for mice with SK-OV-3 xenografts injected with ^{64}Cu-NOTA-F(ab′)$_2$ determined by VOI analysis at baseline, 1 week and 3 weeks after trastuzumab treatment were 3.5 ± 2.6, 6.6 ± 3.7, and 7.4 ± 1.4 %ID/g, respectively. VOI analysis showed an increase in the normalized ratio of %ID/g in the tumor compared to baseline following trastuzumab treatment,

Table 3. Normal tissue distribution of radioactivity at selected times up to 48 h post-injection of ^{64}Cu-NOTA-F(ab′)$_2$ * in non-tumor bearing Balb/c mice.

	Percent injected dose/g (%ID/g)				
Tissue	1 h	3 h	6 h	24 h	48 h
Blood	13.6 ± 0.4	5.5 ± 1.6	1.6 ± 0.1	0.2 ± 0.0	0.2 ± 0.0
Heart	4.0 ± 0.2	3.6 ± 0.9	2.3 ± 0.2	1.0 ± 0.1	0.9 ± 0.1
Lungs	4.9 ± 0.4	4.1 ± 2.2	1.9 ± 0.1	1.3 ± 0.7	1.7 ± 1.2
Liver	6.9 ± 0.6	8.4 ± 2.3	6.3 ± 0.4	4.5 ± 0.6	4.7 ± 0.5
Kidneys	53.8 ± 1.2	81.0 ± 2.3	67.7 ± 5.9	53.6 ± 5.5	45.0 ± 4.0
Spleen	4.9 ± 0.6	7.4 ± 2.4	6.4 ± 0.5	3.6 ± 0.5	3.2 ± 0.5
Stomach	1.4 ± 0.1	1.6 ± 0.5	1.3 ± 0.1	0.7 ± 0.1	0.7 ± 0.1
Intestines	2.8 ± 0.6	2.1 ± 0.8	1.7 ± 0.2	1.0 ± 0.0	1.0 ± 0.1
Muscle	0.5 ± 0.1	0.5 ± 0.1	0.4 ± 0.2	0.2 ± 0.0	0.2 ± 0.0
Bone	2.2 ± 0.5	2.4 ± 1.3	2.2 ± 0.3	1.4 ± 0.2	1.0 ± 0.3
Skin	1.2 ± 0.1	1.8 ± 0.6	1.1 ± 0.3	0.4 ± 0.1	0.3 ± 0.0
Brain	0.4 ± 0.0	0.2 ± 0.1	0.1 ± 0.0	0.1 ± 0.0	0.1 ± 0.0
Ovaries	1.6 ± 0.3	2.3 ± 0.7	1.2 ± 0.2	0.5 ± 0.1	0.5 ± 0.1

Values shown are mean ± SD ($n = 4$).
*Mice were intravenously administered 2–4 MBq (50 μg) of ^{64}Cu-NOTA-pertuzumab F(ab′)$_2$.

Table 4. Radiation absorbed dose projections for ^{64}Cu-NOTA-pertuzumab F(ab′)$_2$ in humans*.

Organ	Equivalent dose (mSv/MBq)
Brain	0.001
Breasts	0.002
Gallbladder wall	0.015
Small intestine	0.011
Lower large intestine	0.282
Heart wall	0.019
Kidneys	1.070
Liver	0.092
Lungs	0.010
Muscle	0.009
Ovaries	0.025
Pancreas	0.016
Spleen	0.068
Total body	0.015

*Radiation absorbed dose projections in humans were based on the cumulative number of disintegrations (N) in source organs in mice obtained from biodistribution studies and were estimated using OLINDA Ver. 1.0 software. This assumes that the relative organ biodistribution of ^{64}Cu-NOTA-pertuzumab F(ab′)$_2$ in humans will be the same as that in mice.

but these values did not reach significance due to variability in this small group size (1.7 ± 0.7, $P = 0.137$ and 1.9 ± 1.4, $P = 0.754$, Fig. 4E). Similarly, SK-OV-3 xenografts clearly exhibited a strong trend toward increased tumor volume over time, despite trastuzumab treatment, but these values did not reach significance due to variability (TGI = 2.2 ± 1.1, $P = 0.109$ at 1 week, 16.5 ± 11.3, $P = 0.124$ at 3 weeks, Fig. 4F).

Discussion

We describe here the construction and characterization of ^{64}Cu-NOTA-pertuzumab F(ab′)$_2$ for PET/CT imaging of the response of HER2-positive tumors to treatment with trastuzumab. MicroPET/CT with ^{64}Cu-NOTA-pertuzumab F(ab′)$_2$ detected decreased HER2 expression in athymic mice engrafted with subcutaneous (s.c.) BT-474 human BC tumors at 1 week after commencing trastuzumab therapy and this was associated with a good response to treatment with trastuzumab (Fig. 4A-C). BT-474 tumor xenografts are sensitive to trastuzumab.[22] In contrast, SK-OV-3 human ovarian cancer xenografts, which overexpress HER2 but are trastuzumab-resistant,[23] demonstrated a 1.9-fold increased uptake of ^{64}Cu-NOTA-pertuzumab F(ab′)$_2$ at 1 and 3 weeks after commencing trastuzumab treatment, and this was associated with continued and rapid tumor growth (Fig. 4D-F). The poor response of SK-OV-3 cells to trastuzumab has been attributed to the absence of the tumor suppressor protein Ras homolog member-1, leading to constitutively phosphorylated MAPK.[24] These results agree with those previously reported by our group for trastuzumab-sensitive MDA-MB-361 human BC xenografts in athymic mice in which microSPECT/CT imaging using ^{111}In-labeled pertuzumab revealed decreased uptake of the imaging probe within 3 days after starting trastuzumab treatment, with almost complete disappearance of tumor accumulation visualized by imaging at 3 weeks post-treatment, which was associated with tumor eradication.[16]

To optimize tumor imaging with ^{64}Cu-NOTA-pertuzumab F(ab′)$_2$, we studied the effect of increasing the administered mass over the range of 5 μg to 200 μg, corresponding to a human mass dose of 5 mg to 400 mg, scaled by body weight (25 g for a mouse vs. 50 kg for a human female). Dijkers et al. reported that a 50 mg mass amount of ^{89}Zr-labeled trastuzumab was optimal for tumor imaging in patients with HER2-positive BC who had not received trastuzumab.[25] Similarly, Mortimer et al. found that pre-administration of 45 mg of trastuzumab prior to ^{64}Cu-labeled trastuzumab (5 mg) for PET decreased liver uptake in patients with HER2-positive BC, but did not diminish tumor uptake.[26] We did not find a significant effect of increasing the mass dose of ^{64}Cu-NOTA-pertuzumab F(ab′)$_2$ on tumor or normal tissue biodistribution at 24 h p.i. in athymic mice with s.c. SK-OV-3 tumor xenografts (Table 2). Wong et al. similarly reported that there was no difference in tumor or liver uptake at 48 h p.i. of 3 μg or 15 μg of ^{86}Y-CHX-A″-panitumumab F(ab′)$_2$ in athymic mice with s.c. epidermal

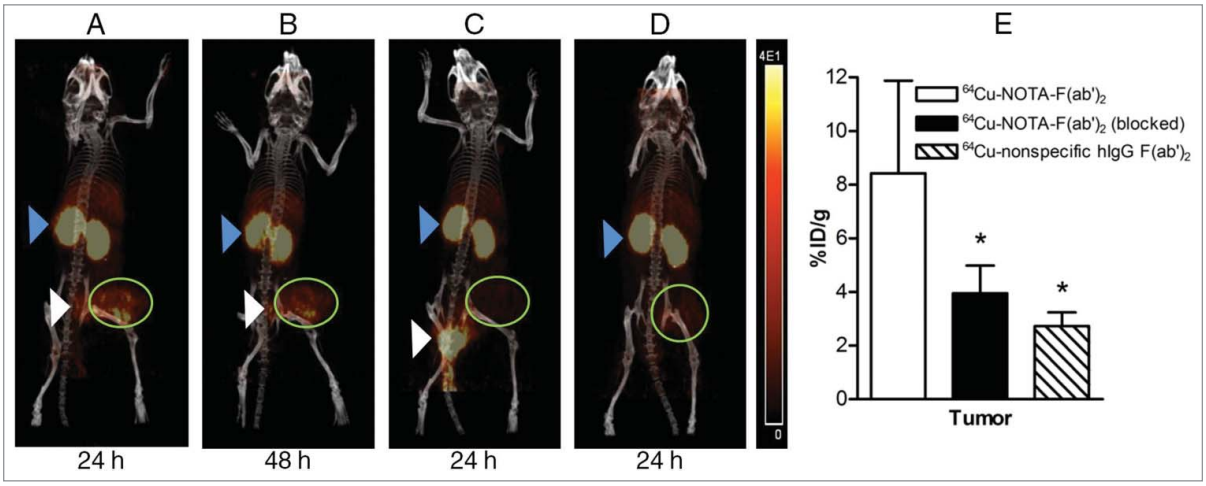

Figure 3. Whole-body microPET/CT images of mice with subcutaneous SK-OV-3 HER2-overexpressing human ovarian cancer xenografts at 24 h post-injection (p.i.) (A) or 48 h p.i. (B) of ^{64}Cu-NOTA-pertuzumab F(ab′)$_2$. (C) Images obtained at 24 h p.i. of ^{64}Cu-NOTA-pertuzumab F(ab′)$_2$ with pre-administration of 1 mg of pertuzumab 24 h prior to radiopharmaceutical injection. (D) Images obtained at 24 h p.i. with ^{64}Cu-labeled nonspecific hIgG F(ab′)$_2$. Tumor xenografts are indicated by the green circle. Also visualized are the kidneys (blue arrowhead) and bladder/urine (white arrowhead). The HER2 specificity of tumor uptake of ^{64}Cu-NOTA-pertuzumab F(ab′)$_2$ was confirmed by biodistribution studies at 48 h p.i. (E) showing a significant decrease in tumor uptake of the radiopharmaceutical in mice pre-administered excess unlabeled pertuzumab to block HER2 or injected with ^{64}Cu-labeled non-specific hIgG F(ab′)$_2$ (*$P < 0.05$).

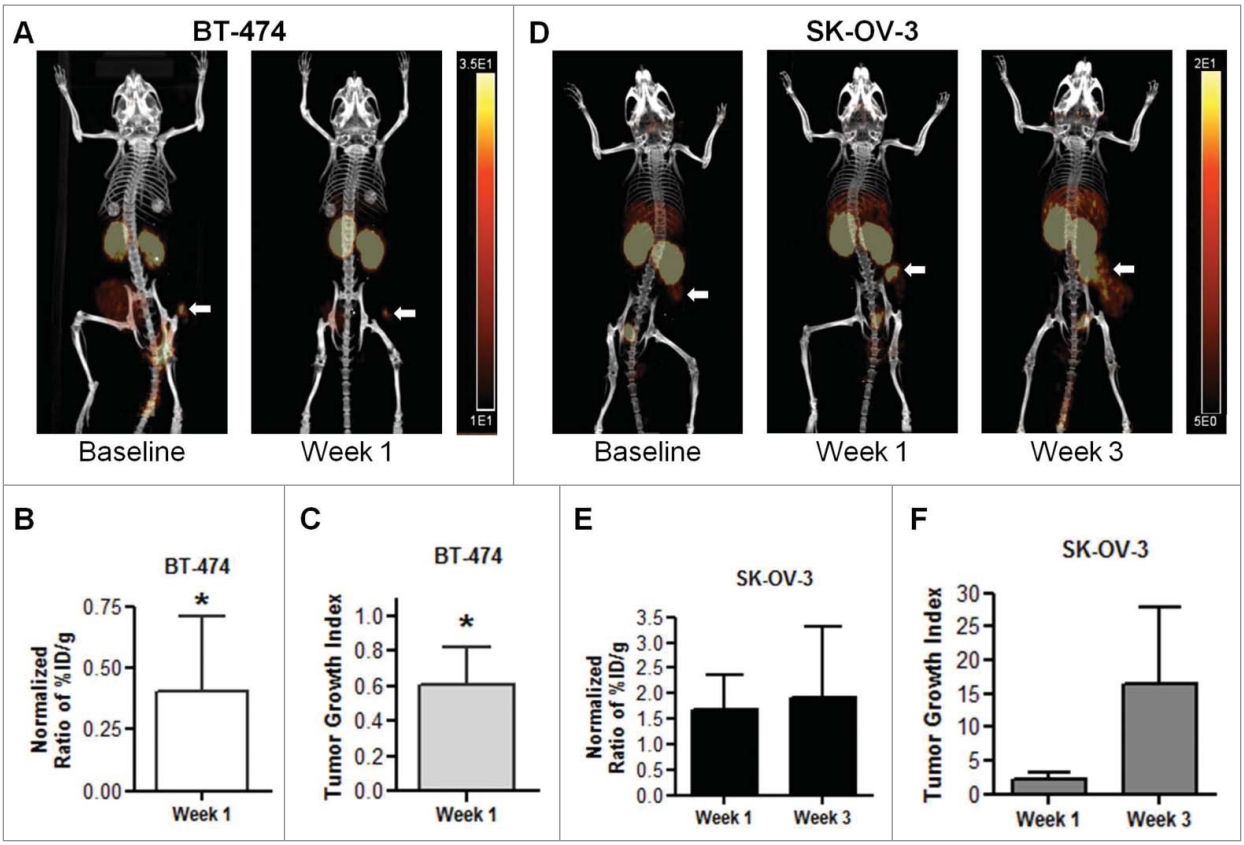

Figure 4. (A) MicroPET/CT images at 24 h post-injection (p.i.) of ^{64}Cu-NOTA-pertuzumab F(ab′)$_2$ in NOD/SCID mice with subcutaneous BT-474 human breast cancer xenografts at baseline and at 1 week after commencing treatment with trastuzumab. (B) The corresponding changes in the ratio of uptake in BT-474 tumors [percent injected dose/g (%ID/g) normalized to the baseline value for each mouse] following injection of ^{64}Cu-NOTA-pertuzumab F(ab′)$_2$ and (C) tumor growth index (TGI). (D) MicroPET/CT images at 24 h p.i. of ^{64}Cu-NOTA-pertuzumab F(ab′)$_2$ in NOD/SCID mice with subcutaneous SK-OV-3 human ovarian cancer xenografts at baseline and at 1 week and 3 weeks after commencing trastuzumab treatment. (E) The corresponding changes in the ratio of SK-OV-3 tumor uptake relative to baseline of ^{64}Cu-NOTA-pertuzumab F(ab′)$_2$ and (F) TGI. Significant differences compared to baseline values are indicated ($^*P < 0.05$).

growth factor receptor-positive LS174T human colon cancer xenografts.[27] In contrast, van Dijk et al. found that mass amounts of 50 μg or more of ^{111}In-cetuximab F(ab′)$_2$ administered to mice with s.c. FaDu squamous cell carcinoma xenografts decreased tumor uptake compared to 10 μg or less, but no differences in liver uptake were noted.[28] The inability to identify a mass effect on liver uptake of ^{64}Cu-NOTA-pertuzumab F(ab′)$_2$ may be related to poor recognition of F(ab′)$_2$ by FcRn receptors.[29] Tumor uptake was moderately high, up to 100 μg of ^{64}Cu-NOTA-pertuzumab F(ab′)$_2$ (Table 2), and there was a trend toward lower tumor uptake at 200 μg. Thus, lower protein amounts may be beneficial, and a 50 μg dose was subsequently used for imaging studies.

Tumor uptake of ^{64}Cu-NOTA-pertuzumab F(ab′)$_2$ (6-10 %ID/g; Table 2) in SK-OV-3 ovarian cancer xenografts at 24 h p.i. was specific, since blocking with an excess of pertuzumab significantly reduced accumulation by 3.7-fold (Fig. 3C) and non-specific ^{64}Cu-NOTA-hIgG F(ab′)$_2$ exhibited 2.2-fold significantly lower uptake (Fig. 3D). The non-specific tumor uptake of ^{64}Cu-NOTA-hIgG F(ab′)$_2$ (Fig. 3D, E) was likely mediated by the enhanced permeability and retention (EPR) effect, which enables accumulation and retention of macromolecules in tumors due to increased vascular permeability and poor lymphatic drainage.[32] Lower tumor uptake of ^{64}Cu-NOTA-pertuzumab F(ab′)$_2$ than previously reported for ^{111}In-labeled pertuzumab IgG was likely due to faster elimination of ^{64}Cu-NOTA-pertuzumab F(ab′)$_2$ from the blood ($t_{1/2}\beta$ = 10.4 h; Fig. 2) compared to ^{111}In-labeled pertuzumab IgG ($t_{1/2}\beta$ = 228.2 h)[18] Tumor uptake of ^{64}Cu-NOTA-pertuzumab F(ab′)$_2$ in SK-OV-3 xenografts was comparable to other radiolabeled F(ab′)$_2$ (7-20 %ID/g).[27,30,31] SK-OV-3 tumors were imaged by microPET/CT at 24 or 48 h p.i. of ^{64}Cu-NOTA-pertuzumab F(ab′)$_2$ (Fig. 3A, B).

The uptake and elimination of ^{64}Cu-NOTA-pertuzumab F(ab′)$_2$ (50 μg) by normal organs in non-tumor bearing Balb/c mice was studied to predict the radiation absorbed doses in humans. There were some differences in normal organ uptake in non-tumor-bearing Balb/c mice (Table 3) at 24 h p.i. of ^{64}Cu-NOTA-pertuzumab F(ab′)$_2$ compared to tumor-bearing Balb/c mice (Table 2). In particular, liver uptake was approximately 2-fold lower and spleen uptake was 3-fold lower in Balb/c than in NOD/SCID mice. The reasons for these differences are not known, but SCID mice have low levels of circulating immunoglobulins which have been shown to influence the pharmacokinetics and spleen uptake of radiolabeled antibodies.[33] The kidneys exhibited the highest normal organ uptake (>80 %ID/g at 3 h p.i. decreasing by 2-fold at 48 h p.i.; Table 3). The kidney uptake at 24 h p.i. (53.6 ± 5.5 %ID/g) in non-tumor-bearing Balb/c mice was not significantly different than in NOD/SCID mice with SK-OV-3 tumors at this time point (65.6 ± 16.2 %ID/g; Table 2). Kidney uptake was much higher than previously observed for ^{64}Cu-NOTA-panitumumab

$F(ab')_2$ (<6 %ID/g).[34] However, kidney uptake of radiolabeled $F(ab')_2$ may depend on the antibody used, since van Dijk et al reported kidney uptake of 17 %ID/g for ^{111}In-labeled cetuximab $F(ab')_2$[35] while Sham J et al. reported 90 %ID/g at 24 h p.i. of ^{89}Zr-labeled αGPC3 $F(ab')_2$.[36] Interestingly, kidney uptake at 24 h p.i. of ^{64}Cu-NOTA-pertuzumab $F(ab')_2$ (65.6 ± 16.2 %ID/g; Table 2) in NOD/SCID mice with SK-OV-3 tumors was identical to that reported by Smith-Jones et al. for ^{111}In-trastuzumab $F(ab')_2$ in athymic mice with BT-474 human BC xenografts (65 %ID/g at 24 h p.i.).[30] Trastuzumab and pertuzumab share human IgG_1 constant domains,[12,37] which may explain the similar kidney uptake of these radiolabeled $F(ab')_2$.

Kidney uptake of antibody fragments is thought to be due to charge interactions of the filtered proteins with renal tubules.[38] Radiation doses projected for administration of ^{64}Cu-NOTA-pertuzumab $F(ab')_2$ to humans revealed that the kidneys would receive the highest dose (1 mSv/MBq) while the total body dose would be 0.015 mSv/MBq (Table 4). The total body dose for ^{64}Cu-NOTA-pertuzumab $F(ab')_2$ is reduced by 3.3-fold compared to ^{111}In-labeled pertuzumab IgG (0.05 mSv/MBq),[18] but the dose to the kidneys is increased by 3-fold (1 mSv/MBq vs. 0.33 mSv/MBq). Since Phase 1 clinical trials of ^{64}Cu-labeled trastuzumab for PET imaging of HER2-positive BC have used administered amounts as low as 115 MBq,[39] we project that the total body dose for a single injection of ^{64}Cu-NOTA-pertuzumab $F(ab')_2$ would be 1.7 mSv at this amount, and for the 3 administrations used for the baseline, 1 week and 4 weeks imaging studies in the PETRA trial, would be 5.1 mSv. This compares to 17 mSv for ^{111}In-labeled pertuzumab, thus the radiation dose to patients would be reduced by more than 3-fold. The dose to the kidneys assuming 3 administrations (115 MBq each) of ^{64}Cu-NOTA-pertuzumab $F(ab')_2$ would be 115 mSv. There is no safety risk at these radiation doses to the kidneys, since they represent <0.5% of the maximally-tolerated dose for the kidneys (23-25 Sv).[40] Moreover, ^{111}In-pentetreotide, which is a clinically used radiopeptide for imaging somatostatin receptor-positive neuroendocrine malignancies in humans, deposits a similar radiation dose of 108 mSv in the kidneys from administration of a single dose of 222 MBq.[41]

In conclusion, we demonstrated that ^{64}Cu-NOTA-pertuzumab $F(ab')_2$ specifically target HER2 on BC tumor xenografts in NOD/SCID mice and that microPET/CT can detect changes in HER2 expression associated with response to trastuzumab treatment. Organ absorbed doses associated with ^{64}Cu-NOTA-pertuzumab $F(ab')_2$ in humans are projected to be lower than those of ^{111}In-BzDTPA-pertuzumab with the exception of the kidneys and lower large intestine.

Materials and methods

Cells lines and tumor xenografts

SK-BR-3 human breast cancer (BC) cells and SK-OV-3 human ovarian cancer cells, both expressing 1–2 × 10^6 HER2/cell[42,43] were cultured in RPMI 1640 (Sigma-Aldrich #R8758) supplemented with 10% fetal bovine serum (FBS, Life Technologies #12484028). BT-474 human BC cells (1–2 × 10^6 HER2/cell)[44] were grown in Dulbecco Modified Eagle Medium (University Health Network) supplemented with 10% FBS. All cells were cultured at 37°C/5% CO_2. Female NOD/SCID mice (Ontario Cancer Institute) were inoculated s.c. with 1 × 10^7 SK-OV-3 or BT-474 cells in 200 μL of serum free medium or a 1:1 mixture of Matrigel (Corning #CACB354234) and medium. Mice were implanted with a 0.72 mg 60 days sustained release 17β-estradiol pellet (Innovative Research of America #SE-121) at 24 h prior to inoculation of BT-474 cells, which is required for growth of these tumors in NOD/SCID mice.

Pertuzumab $F(ab')_2$

Pertuzumab $F(ab')_2$ were generated by pre-equilibrating 625 μL of immobilized pepsin slurry (Thermo Scientific #20343) with 20 mM sodium acetate trihydrate buffer, pH 4.5 (500 μL) and then adding 10 mg of pertuzumab IgG ($M_r \approx 148$ kDa; Genentech) prepared in 1 mL of the same buffer. The mixture was incubated at 37°C on an end-over-end mixer for 5.5 h and then centrifuged at 1000 × *g* for 5 min. The supernatant was collected and the resin was rinsed twice by resuspending in 750 μL phosphate buffered saline (PBS, pH 7.4), centrifuging again, collecting and pooling the washes, and then passing the pooled volume through a Millex-GV PVDF 0.22 μm filter (EMD Millipore #SLGV033SL). Completion of digestion of IgG to $F(ab')_2$ was assessed by sodium dodecyl sulfate polyacrylamide gel electrophoresis (SDS-PAGE) on a 4–20% Tris HCl gradient gel (Bio-Rad #456-1093) stained with Coomassie G-250 stain (Bio-Rad #161-0786). If digestion was not complete, the pooled supernatant was applied to a NAb Protein A agarose spin column (Thermo Scientific #89956) equilibrated with PBS (pH 7.4), and then incubated for 10 min at room temperature (RT) on an end-over-end mixer to bind IgG. The column was centrifuged at 1000 × *g* for 1 min and the flow-through containing the $F(ab')_2$ was collected. The column was washed twice by adding 1 mL of PBS, centrifuging, and collecting the wash fractions. Pertuzumab $F(ab')_2$ were evaluated for purity by SDS-PAGE on a 4–20% gel stained with Coomassie G-250 blue dye. Additionally, size-exclusion high performance liquid chromatography (SE-HPLC) was conducted on a BioSep SEC-S2000 column (Phenomenex) eluted with 0.1 M NaH_2PO_4 buffer (pH 7.0) at a flow rate of 0.8 mL/min and monitored with a diode array UV detector at 280 nm (PerkinElmer). $F(ab')_2$ of non-specific human IgG (hIgG) from human serum (Sigma-Aldrich #I4506) were similarly prepared and analyzed for purity.

Preparation of ^{64}Cu-NOTA-pertuzumab $F(ab')_2$

Pertuzumab $F(ab')_2$ were buffer-exchanged and concentrated to 2.5, 5 or 10 mg/mL in 0.1 M $NaHCO_3$, pH 9.0, in an Amicon Ultra device (Millipore #UFC503096; M_r cut-off = 30 kDa). Protein concentration was determined spectrophotometrically [$E_{280nm} = 1.5$ (mg/mL)$^{-1}$cm^{-1}]. $F(ab')_2$ (2.5, 5 or 10 mg/mL) were modified with NOTA for complexing ^{64}Cu by reaction with a 5-fold or 10-fold molar excess of 2-S-(4-isothiocyanatobenzyl)-1,4,7-triazacyclononane-1,4,7-triaceticacid (*p*-SCN-Bn-NOTA; Macrocyclics #B605) for 2 h at RT. The *p*-SCN-Bn-NOTA was dissolved in 5 μL dimethyl sulfoxide, incubated for 10 min at 37°C to facilitate dissolution, and then diluted to a concentration

of 1.5 mg/mL in 0.1 M $NaHCO_3$, pH 9.0. NOTA-pertuzumab $F(ab')_2$ were purified from unconjugated NOTA by ultracentrifugation with 0.1 M CH_3CO_2Na buffer, pH 5.5, in an Amicon Ultra device (M_r cut-off = 30 kDa). NOTA-pertuzumab $F(ab')_2$ concentration was determined with the Bradford Assay using Pierce Coomassie Plus Assay Reagent (Thermo Scientific #23238). The NOTA substitution level of the $F(ab')_2$ was measured by labeling an aliquot of the unpurified conjugation mixture with ^{64}Cu, then determining the proportion of ^{64}Cu-NOTA-pertuzumab $F(ab')_2$ vs. ^{64}Cu-NOTA by instant thin-layer silica gel chromatography (ITLC-SG; Agilent Technologies #SGI0001) and multiplying this fraction by the molar ratio used in the reaction. To enable ^{64}Cu labeling, sufficient 0.1 M CH_3CO_2Na buffer, pH 5.5 was added to the labeling mixture to assure that the final pH was pH 5.5 (confirmed using pH paper). An alternative novel spectrophotometric assay to measure and verify substitution level was also developed. For this assay, the UV absorbance of the NOTA-$F(ab')_2$ conjugate was measured at 280 nm. The absorbance contribution from the $F(ab')_2$ was determined by comparing the known protein concentration of $F(ab')_2$ (Bradford Assay) to a standard curve of UV absorbance at 280 nm vs. $F(ab')_2$ concentration. The difference in absorbance between the NOTA-$F(ab')_2$ conjugate and that contributed by $F(ab')_2$ was attributable to NOTA. NOTA concentration was derived by reference to a standard curve of UV absorbance at 280 nm vs. NOTA concentration. The ratio of NOTA concentration to $F(ab')_2$ concentration yielded the substitution level. Purity and homogeneity of the optimized NOTA-pertuzumab $F(ab')_2$ conjugates were assessed by SDS-PAGE and SE-HPLC as described above. Radiolabeling of NOTA-pertuzumab $F(ab')_2$ with ^{64}Cu was achieved by incubation for 1 h at 40°C with $^{64}CuCl_2$ (Washington University, St. Louis, MO) in 0.1 M CH_3CO_2Na buffer, pH 5.5 to achieve a specific activity of 370 kBq/μg for general procedures or 2.6 MBq/μg for imaging studies. ^{64}Cu-NOTA-pertuzumab $F(ab')_2$ was purified in an Amicon Ultra device (M_r cut-off = 30 kDa). The final radiochemical purity was determined by ITLC-SG developed in 0.1 M sodium citrate, pH 5.0 and by SE-HPLC using a Flow Scintillation Analyzer (FSA) radioactivity detector (PerkinElmer). The R_f values for ^{64}Cu-NOTA-$F(ab')_2$ on ITLC were 0.0 and those for ^{64}Cu-NOTA and free ^{64}Cu were 0.8–0.9 and 1.0, respectively. $F(ab')_2$ of non-specific hIgG were similarly modified with NOTA and labeled with ^{64}Cu. Trace metals were removed from all buffers using Chelex-100 cation-exchange resin (Bio-Rad #142-2832).

HER2 binding and trastuzumab-mediated HER2 internalization

The binding of ^{64}Cu-NOTA-pertuzumab $F(ab')_2$ to HER2 on SK-BR-3 cells (1–2 × 10^6 HER2/cell) was determined by saturation radioligand binding assays.[42] Increasing concentrations of ^{64}Cu-NOTA-pertuzumab $F(ab')_2$ (0.07 to 300 nM) were incubated with 1 × 10^6 SK-BR-3 cells in 1.5 mL microcentrifuge tubes in PBS in the presence [non-specific binding (NSB)] or absence [total binding (TB)] of 61 μM of unlabeled pertuzumab. The tubes were incubated at 4°C for 3.5 h with occasional shaking, then centrifuged at 420 × g for 5 min and the supernatant and cell pellet separated and measured in a γ-counter. Specific binding (SB) was calculated by subtracting NSB from TB and plotted vs. the unbound concentration of ^{64}Cu-NOTA-$F(ab')_2$. The resulting curve was fitted to a 1-site receptor-binding model by Prism Ver. 4.0 software (GraphPad) and the dissociation constant (K_d) and maximum number of receptors/cell (B_{max}) estimated.

Single concentration radioligand binding assays with ^{64}Cu-NOTA-pertuzumab $F(ab')_2$ were performed to assess trastuzumab-mediated HER2 internalization in SK-OV-3 or BT-474 cells. Briefly, 4 × 10^5 SK-OV-3 or 3 × 10^5 BT-474 cells were seeded in 6-well plates and cultured overnight. The medium was removed and the cells incubated at 37°C for 24 h with trastuzumab (14 μg/mL) in 2 mL of fresh medium or medium alone. The medium was again removed and rinsed with PBS, pH 7.3. The cells were then incubated with 10 nM ^{64}Cu-NOTA-pertuzumab $F(ab')_2$ in the absence or presence of a 50-fold excess of pertuzumab in PBS, pH 7.3 for 3 h at 4°C to measure TB and NSB. The medium was removed, and the cells were rinsed twice with PBS, pH 7.3 and then solubilized in 100 mM NaOH. The solubilized cells were transferred to γ-counting tubes and the cell-bound radioactivity measured in a γ-counter. SB was calculated by subtracting NSB from TB. The percent change in HER2 expression was calculated by comparing the SB of trastuzumab treated cells to the SB of untreated cells.

Biodistribution, pharmacokinetic and radiation dosimetry studies

To evaluate the effect of the administered mass of ^{64}Cu-NOTA-$F(ab')_2$ on tumor and normal tissue uptake, SK-OV-3 tumor-bearing mice were injected i.v. (tail vein) with 5, 50, 100, or 200 μg labeled with 1–3 MBq of ^{64}Cu. Mice were sacrificed at 24 h post-injection (p.i.), and tumors and selected normal tissues were collected, weighed and counted, along with a standard of the injected radioactivity, in a γ-counter. Tumor and normal tissue uptake were expressed as percentage injected dose per gram (%ID/g). The 24 h time point was chosen based on a previous study with ^{111}In-DOTA-trastuzumab $F(ab')_2$ that showed maximal tumor uptake was achieved at 24 h p.i.[30]

The radioactivity in the blood and normal tissues at 1, 3, 6, 24, and 48 h post-injection was determined in groups of 4 non-tumor bearing female Balb/c mice (Charles River) following i.v. injection of ^{64}Cu-NOTA-pertuzumab $F(ab')_2$ (50 μg; 2–4 MBq). In addition, the pharmacokinetics of elimination of ^{64}Cu-NOTA-pertuzumab $F(ab')_2$ from the blood of Balb/c mice were determined by plotting the radioactivity (%ID/mL) vs. time post-injection, and fitting the curve to a 2-compartment pharmacokinetic model using Scientist® Ver. 2.01 software (MicroMath Scientific Software). Standard pharmacokinetic parameters were estimated.

Radiation absorbed doses to normal organs were estimated as previously described.[18] Briefly, the dose to target organs was estimated as D = N × DF, where N is the number of disintegrations (Bq × h/Bq) in a source organ, and DF is the Dose Factor using the RAdiation Dose Assessment Resource (RADAR) formalism. The number of disintegrations ($N_{0\text{-}48h}$) from 0 h to 48 h p.i. of ^{64}Cu-NOTA-pertuzumab $F(ab')_2$ was estimated by first integrating the area-under-the-curve (AUC) for the radioactivity (not corrected for decay) vs. time plot for

each source organ. The AUC from 48 h to infinity ($N_{48h-\infty}$) was estimated by dividing the radioactivity in the source organ at 48 h by the decay constant for ^{64}Cu (0.05457 h^{-1}), thus assuming further elimination only by radioactive decay. The total AUC ($N_{0-\infty}$) was the sum of $N_{0-48\ h}$ and $N_{48h-\infty}$ and was then divided by the injected amount of radioactivity (Bq) to yield the total number of disintegrations for input into OLINDA/EXM 1.0 radiation dosimetry software for prediction of the radiation absorbed doses to target organs in humans.[45]

All animal studies were conducted under a protocol (no. 4336.0) approved by the Animal Care Committee at the University Health Network in accordance with Canadian Council on Animal Care guidelines.

MicroPET/CT imaging studies

For microPET/CT imaging, groups of 3-4 mice with s.c. SK-OV-3 tumors were injected i.v. with ^{64}Cu-NOTA-pertuzumab F(ab′)$_2$ (50 μg; 10–11 MBq) or ^{64}Cu-labeled non-specific hIgG F(ab′)$_2$ [^{64}Cu-NOTA-hIgG F(ab′)$_2$; 50 μg; 6–10 MBq]. To further assess the specificity of tumor uptake, some groups of mice received an intraperitoneal (i.p.) injection of 1 mg of pertuzumab 24 h prior to ^{64}Cu-NOTA-pertuzumab F(ab′)$_2$. Mice were sedated with isoflurane and imaged with a microPET tomograph (Siemens MicroPet Focus 220) and CT scanner (GE Locus Ultra) at 24 and 48 h post-injection. MicroPET images were acquired with a 350–650 keV window for 20–75 min with a coincidence timing window of 6 ns. Image reconstruction was achieved using ordered subset expectation maximization (OSEM), followed by a maximum *a posterior* probability reconstruction algorithm with no correction for attenuation or partial-volume effects (PVE). The full width at half maximum (FWHM) resolution of the microPET is 1.6 mm. Soret et al. discuss that the PVE results in inaccuracy in quantitation of radioactivity uptake mostly for tumors with diameter less than 2–3 times the FWHM of the PET tomograph.[46] The tumors in our study were >4–5 mm in diameter, which exceeds 2–3 times the FWHM of the microPET system (1.6 mm). Following microPET imaging, mice were immediately transferred to an eXplore Locus Ultra Preclinical CT scanner (GE Healthcare) for a whole body CT scan using routine acquisition parameters (80 kVp, 50 mA, and voxel size of 154 × 154 × 154 μm). MicroPET and CT images were processed using Inveon Research Workplace software (Siemens). Immediately after CT imaging, mice were sacrificed and the 48 h biodistribution determined as described above.

To study the utility of microPET/CT imaging with ^{64}Cu-NOTA-pertuzumab F(ab′)$_2$ to detect HER2 internalization in tumors associated with response to treatment with trastuzumab,[16] groups of 3–6 athymic mice bearing SK-OV-3 or BT-474 tumor xenografts were injected with ^{64}Cu-NOTA-pertuzumab F(ab′)$_2$ (50 μg; 7–13 MBq). Images were obtained at 24 h p.i. to obtain baseline tumor uptake of ^{64}Cu-NOTA-pertuzumab F(ab′)$_2$. Mice were then treated with trastuzumab administered i.p. 2 days later using a loading dose of 4 mg/kg followed by weekly doses of 2 mg/kg for 2 weeks, diluted in normal saline to a volume of 100 μL. We previously found that i.p. administration of ^{111}In-labeled trastuzumab provides 70% bioavailability relative to i.v. (tail vein) injection in athymic mice.[47] Assessment of HER2 internalization was performed by repeating the injection of ^{64}Cu-NOTA-pertuzumab F(ab′)$_2$ at 1 week and 3 weeks and re-acquiring microPET/CT images at 24 h p.i. Tumor response to trastuzumab was assessed by weekly measurements of tumor length and width using calipers and calculating tumor volume as $V = length \times width^2 \times 0.5$. A tumor growth index (TGI) was derived by dividing the measured tumor volume by the initial volume prior to trastuzumab treatment. Quantification of tumor uptake on the pre- and post-treatment images was performed by region-of-interest (ROI) analysis using Inveon Research Workplace software (Siemens) and tumor uptake was expressed as %ID/g. Changes in tumor uptake were normalized for each mouse by dividing the %ID/g values at 1-week or 3-weeks after commencing trastuzumab treatment by the baseline value prior to treatment.

Statistical analysis

Results were expressed as mean ± SD and tested for statistical significance using a one way ANOVA (F-test) or 2-sided Student's t-test and SPSS version 17.0 software (IBM). The level of significance was set at $P < 0.05$. Response to trastuzumab treatment as measured by tumor uptake of ^{64}Cu-NOTA-pertuzumab F(ab′)$_2$ over time was compared by a paired *t* test.

Disclosure of potential conflicts of interest

Pertuzumab was provided by Genentech, Inc. (San Francisco, CA) for this study through a Materials Transfer Agreement with the University of Toronto (Raymond Reilly).

Acknowledgments

This study was supported by grants from the Smarter Imaging Program of the Ontario Institute for Cancer Research with funds from the Province of Ontario. K. Lam received the MDS-Nordion Graduate Scholarship in Radiopharmaceutical Sciences and the Edward A. Simmons PhmB 1919 Pharmacy Fellowship. Parts of this research were presented at the 18th European Symposium on Radiopharmacy and Radiopharmaceuticals in Salzburg, Austria, April 7–10, 2016. The authors thank Michael Dunne for his assistance with the pharmacokinetic analyses. The authors would also like to thank Deborah A. Scollard and Teesha Komal of the STTARR (Spatio-temporal Targeting and Amplification of Radiation Response) center for assisting with PET/CT imaging.

References

1. Ross JS, Slodkowska EA, Symmans WF, Pusztai L, Ravdin PM, Hortobagyi GN. The HER-2 receptor and breast cancer: ten years of targeted anti-HER-2 therapy and personalized medicine. Oncologist 2009; 14:320-68; PMID:19346299; http://dx.doi.org/10.1634/theoncologist.2008-0230
2. Slamon DJ, Clark GM, Wong SG, Levin WJ, Ulrich A, McGuire WL. Human breast cancer: Correlation of relapse and survival with amplification of the HER-2/neu oncogene. Science 1987; 235:177-82; PMID:3798106; http://dx.doi.org/10.1126/science.3798106
3. Andrulis IL, Bull SB, Blackstein ME, Sutherland D, Mak C, Sidlofsky S, Pritzker KP, Hartwick RW, Hanna W, Lickley L, et al. neu/erbB-2 Amplification identifies a poor-prognosis group of women with node-negative breast cancer. J Clin Oncol 1998; 16:1340-9; PMID:9552035; http://dx.doi.org/10.1200/jco.1998.16.4.1340
4. Slamon DJ, Leyland-Jones B, Shak S, Fuchs H, Paton V, Bajamonde A, Fleming T, Eiermann W, Wolter J, Pegram M, et al. Use of chemotherapy plus a monoclonal antibody against HER2 for metastatic breast

cancer that overexpresses HER2. N Engl J Med 2001; 344:783-92; PMID:11248153; http://dx.doi.org/10.1056/NEJM200103153441101
5. Romond EH, Perez EA, Bryant J, Suman VJ, Geyer CE, Jr., Davidson NE, Tan-Chiu E, Martino S, Paik S, Kaufman PA, et al. Trastuzumab plus adjuvant chemotherapy for operable HER2-positive breast cancer. N Engl J Med 2005; 353:1673-84; PMID:16236738; http://dx.doi.org/10.1056/NEJMoa052122
6. Piccart-Gebhart MJ, Procter M, Leyland-Jones B, Goldhirsch A, Untch M, Smith I, Gianni L, Baselga J, Bell R, Jackisch C, et al. Trastuzumab after adjuvant chemotherapy in HER2-positive breast cancer. N Engl J Med 2005; 353:1659-72; PMID:16236737; http://dx.doi.org/10.1056/NEJMoa052306
7. Wolff AC, Hammond ME, Hicks DG, Dowsett M, McShane LM, Allison KH, Allred DC, Bartlett JM, Bilous M, Fitzgibbons P, et al. Recommendations for human epidermal growth factor receptor 2 testing in breast cancer: American Society of Clinical Oncology/College of American Pathologists Clinical practice guideline update. J Clin Oncol 2013; PMID:24101045; http://dx.doi.org/10.1200/JCO.2013.50.9984
8. Nahta R, Esteva FJ. Herceptin: mechanisms of action and resistance. Cancer Lett 2006; 232:123-38; PMID:16458110; http://dx.doi.org/10.1016/j.canlet.2005.01.041
9. Paik S, Kim C, Wolmark N. HER2 status and benefit from adjuvant trastuzumab in breast cancer. N Engl J Med 2008; 358:1409-11; PMID:18367751; http://dx.doi.org/10.1056/NEJMc0801440
10. McLarty K, Reilly RM. Molecular imaging as a tool for personalized and targeted anticancer therapy. Clin Pharmacol Ther 2007; 81:420-4; PMID:17339871; http://dx.doi.org/10.1038/sj.clpt.6100096
11. Cuello M, Ettenberg AA, Clark AS, Keane MM, Posner RH, Nau MM, Dennis PA, Lipkowitz S. Down-regulation of the erbB-2 receptor by trastuzumab (Herceptin) enhances tumor necrosis factor-related apoptosis-inducing ligand-mediated apoptosis in breast and ovarian cancer cell lines that overexpress erbB-2. Cancer Res 2001; 61:4892-900; PMID:11406568
12. Adams CW, Allison DE, Flagella K, Presta L, Clarke J, Dybdal N, McKeever K, Sliwkowski MX. Humanization of a recombinant monoclonal antibody to produce a therapeutic HER dimerization inhibitor, pertuzumab. Cancer Immunol Immunother 2006; 55:717-27; PMID:16151804; http://dx.doi.org/10.1007/s00262-005-0058-x
13. Vu T, Claret FX. Trastuzumab: updated mechanisms of action and resistance in breast cancer. Front Oncol 2012; 2:62; PMID:22720269; http://dx.doi.org/10.3389/fonc.2012.00062
14. Swain SM, Kim SB, Cortés J, Ro J, Semiglazov V, Campone M, Ciruelos E, Ferrero JM, Schneeweiss A, Knott A, et al. Pertuzumab, trastuzumab, and docetaxel for HER2-positive metastatic breast cancer (CLEOPATRA study): overall survival results from a randomised, double-blind, placebo-controlled, phase 3 study. Lancet Oncol 2013; 14:461-71; PMID:23602601; http://dx.doi.org/10.1016/S1470-2045(13)70130-X
15. Gianni L, Pienkowski T, Im YH, Roman L, Tseng LM, Liu MC, Lluch A, Staroslawska E, de la Haba-Rodriguez J, Im SA, et al. Efficacy and safety of neoadjuvant pertuzumab and trastuzumab in women with locally advanced, inflammatory, or early HER2-positive breast cancer (NeoSphere): a randomised multicentre, open-label, phase 2 trial. Lancet Oncol 2012; 13:25-32; PMID:22153890; http://dx.doi.org/10.1016/S1470-2045(11)70336-9
16. McLarty K, Cornelissen B, Cai Z, Scollard DA, Costantini DL, Done SJ, Reilly RM. Micro-SPECT/CT with ^{111}In-DTPA-pertuzumab sensitively detects trastuzumab-mediated HER2 downregulation and tumor response in athymic mice bearing MDA-MB-361 human breast cancer xenografts. J Nucl Med 2009; 50:1340-8; PMID:19617342; http://dx.doi.org/10.2967/jnumed.109.062224
17. Lam K, Scollard DA, Chan C, Levine MN, Reilly RM. Kit for the preparation of ^{111}In-labeled pertuzumab injection for imaging response of HER2-positive breast cancer to trastuzumab (Herceptin). Appl Radiat Isot 2014; 95C:135-42; PMID:25464190; http://dx.doi.org/10.1016/j.apradiso.2014.10.011
18. Lam K, Chan C, Done SJ, Levine MN, Reilly RM. Preclinical pharmacokinetics, biodistribution, radiation dosimetry and acute toxicity studies required for regulatory approval of a Clinical Trial Application for a Phase I/II clinical trial of ^{111}In-BzDTPA-pertuzumab. Nucl Med Biol 2015; 42:78-84; PMID:25459109; http://dx.doi.org/10.1016/j.nucmedbio.2014.09.011
19. Rahmim A, Zaidi H. PET versus SPECT: strengths, limitations and challenges. Nucl Med Commun 2008; 29:193-207; PMID:18349789; http://dx.doi.org/10.1097/MNM.0b013e3282f3a515; http://dx.doi.org/10.1097/MNM.0b013e3282f3a515
20. McCarthy DW, Shefer RE, Klinkowstein RE, Bass LA, Margeneau WH, Cutler CS, Anderson CJ, Welch MJ. Efficient production of high specific activity ^{64}Cu using a biomedical cyclotron. Nucl Med Biol 1997; 24:35-43; PMID:9080473; http://dx.doi.org/10.1016/S0969-8051(96)00157-6
21. Reilly RM. The radiochemistry of monoclonal antibodies and peptides. In: Reilly RM, ed. Monoclonal Antibody and Peptide-Targeted Radiotherapy of Cancer. Hoboken, NJ: John Wiley & Sons., 2010:39-100; http://dx.doi.org/10.1002/9780470613214
22. Baselga J, Norton L, Albanell J, Kim YM, Mendelsohn J. Recombinant humanized anti-HER2 antibody (Herceptin) enhances the antitumor activity of paclitaxel and doxorubicin against HER2/neu overexpressing human breast cancer xenografts. Cancer Res 1998; 58:2825-31; PMID:9661897
23. Wilken JA, Webster KT, Maihle NJ. Trastuzumab Sensitizes Ovarian Cancer Cells to EGFR-targeted Therapeutics. J Ovarian Res 2010; 3:7; PMID:20346177; http://dx.doi.org/10.1186/1757-2215-3-7
24. Longva KE, Pedersen NM, Haslekas C, Stang E, Madshus IH. Herceptin-induced inhibition of ErbB2 signaling involves reduced phosphorylation of Akt but not endocytic down-regulation of ErbB2. Int J Cancer 2005; 116:359-67; PMID:15800944; http://dx.doi.org/10.1002/ijc.21015
25. Dijkers EC, Oude Munnink TH, Kosterink JG, Brouwers AH, Jager PL, de Jong JR, van Dongen GA, Shröder CP, Lub-de Hooge MN, de Vries EG. Biodistribution of ^{89}Zr-trastuzumab and PET imaging of HER2-positive lesions in patients with metastatic breast cancer. Clin Pharmacol Ther 2010; 87:586-92; PMID:20357763; http://dx.doi.org/10.1038/clpt.2010.12
26. Mortimer JE, Bading JR, Colcher DM, Conti PS, Frankel PH, Carroll MI, Tong S, Poku E, Miles JK, Shively JE, et al. Functional imaging of human epidermal growth factor receptor 2-positive metastatic breast cancer using (64)Cu-DOTA-trastuzumab PET. J Nucl Med 2014; 55:23-29; PMID:24337604; http://dx.doi.org/10.2967/jnumed.113.122630
27. Wong KJ, Baidoo KE, Nayak TK, Garmestani K, Brechbiel MW, Milenic DE. In vitro and in vivo pre-clinical analysis of a F(ab′)$_2$ fragment of panitumumab for molecular imaging and therapy of HER1 positive cancers. EJNMMI Res 2011; 1; PMID:21845232; http://dx.doi.org/10.1186/2191-219X-1-1
28. van Dijk LK, Hoeben BA, Kaanders JH, Franssen GM, Boerman OC, Bussink J. Imaging of epidermal growth factor receptor expression in head and neck cancer with SPECT/CT and ^{111}In-labeled cetuximab-F(ab′)$_2$. J Nucl Med 2013; 54:2118-24; PMID:24136932; http://dx.doi.org/10.2967/jnumed.113.123612
29. Mould DR, Sweeney KR. The pharmacokinetics and pharmacodynamics of monoclonal antibodies–mechanistic modeling applied to drug development. Curr Opin Drug Discov Devel 2007; 10:84-96; PMID:17265746
30. Smith-Jones PM, Solit DB, Akhurst T, Afroze F, Rosen N, Larson SM. Imaging the pharmacodynamics of HER-2 degradation in response to Hsp90 inhibitors. Nat Biotechnol 2004; 22:701-6; PMID:15133471; http://dx.doi.org/10.1038/nbt968
31. Oude Munnink TH, de Vries EG, Vedelaar SR, Timmer-Bosscha H, Schroder CP, Brouwers AH, Lub-de Hooge MN. Lapatinib and 17AAG reduce ^{89}Zr-trastuzumab-F(ab′)$_2$ uptake in SKBR3 tumor xenografts. Mol Pharm 2012; 9:2995-3002; PMID:23003202; http://dx.doi.org/10.1021/mp3002182
32. Maeda H, Wu J, Sawa T, Matsumura Y, Hori K. Tumor vascular permeability and the EPR effect in macromolecular therapeutics: a review. J Control Release 2000; 65:271-84. PMID:10699287; http://dx.doi.org/10.1016/S0168-3659(99)00248-5
33. Michel RB, Ochakovskaya R, Mattes MJ. Rapid blood clearance of injected mouse IgG2a in SCID mice. Cancer Immunol Immunother 2002; 51:547-56. PMID:12384806; http://dx.doi.org/10.1007/s00262-002-0319-x

34. Boyle AJ, Cao PJ, Hedley DW, Sidhu SS, Winnik MA, Reilly RM. MicroPET/CT imaging of patient-derived pancreatic cancer xenografts implanted subcutaneously or orthotopically in NOD-scid mice using (64)Cu-NOTA-panitumumab F(ab′)2 fragments. Nucl Med Biol 2015; 42:71-7; PMID:25456837; http://dx.doi.org/10.1016/j.nucmedbio.2014.10.009
35. van Dijk LK, Boerman OC, Franssen GM, Kaanders JH, Bussink J. ^{111}In-cetuximab-F(ab′)$_2$ SPECT and 18F-FDG PET for prediction and response monitoring of combined-modality treatment of human head and neck carcinomas in a mouse model. J Nucl Med 2015; 56:287-92. PMID:25552666; http://dx.doi.org/10.2967/jnumed.114.148296
36. Sham JG, Kievit FM, Grierson JR, Miyaoka RS, Yeh MM, Zhang M, et al. Glypican-3-targeted 89Zr PET imaging of hepatocellular carcinoma. J Nucl Med 2014; 55:799-804. PMID:24627434; http://dx.doi.org/10.2967/jnumed.113.132118
37. Carter P, Presta L, Gorman CM, Ridgway JB, Henner D, Wong WL, Rowland AM, Kotts C, Carver ME, Shepard HM. Humanization of an anti-p185 HER2 antibody for human cancer therapy. Proc Natl Acad Sci USA 1992; 89:4285-9; PMID:1350088; http://dx.doi.org/10.1073/pnas.89.10.4285
38. Behr TM, Sharkey RM, Juweid ME, Blumenthal RD, Dunn RM, Griffiths GL, Bair HJ, Wolf FG, Becker WS, Goldenberg DM. Reduction of the renal uptake of radiolabeled monoclonal antibody fragments by cationic amino acids and their derivatives. Cancer Res 1995; 55:3825-34; PMID:7641200
39. Tamura K, Kurihara H, Yonemori K, Tsuda H, Suzuki J, Kono Y, Honda N, Kodaira M, Yamamoto H, Yunokawa M, et al. ^{64}Cu-DOTA-trastuzumab PET imaging in patients with HER2-positive breast cancer. J Nucl Med 2013; 54:1869-75; PMID:24029656; http://dx.doi.org/10.2967/jnumed.112.118612
40. Emami B, Lyman J, Brown A, Coia L, Goitein M, Munzenrider JE, Shank B, Solin LJ, Wesson M. Tolerance of normal tissue to therapeutic irradiation. Int J Radiat Oncol Biol Phys 1991; 21:109-22; PMID:2032882; http://dx.doi.org/10.1016/0360-3016(91)90171-Y
41. Anonymous. Octreoscan Kit for the preparation of indium-111 pentetreotide. St. Louis, MO: Mallinckrodt Medical Inc., 2015.
42. McLarty K, Cornelissen B, Scollard DA, Done SJ, Chun K, Reilly RM. Associations between the uptake of ^{111}In-DTPA-trastuzumab, HER2 density and response to trastuzumab (Herceptin) in athymic mice bearing subcutaneous human tumour xenografts. Eur J Nucl Med Mol Imaging 2009; 36:81-93; PMID:18712381; http://dx.doi.org/10.1007/s00259-008-0923-x
43. Chan C, Scollard, DA, McLarty, K, Smith, S, Reilly, RM. A comparison of ^{111}In- or ^{64}Cu-DOTA-trastuzumab Fab fragments for imaging subcutaneous HER2-positive tumor xenografts in athymic mice using microSPECT/CT or microPET/CT. EJNMMI Res 2011; 1:15; PMID:22214307; http://dx.doi.org/10.1186/2191-219X-1-15
44. Tang Y, Wang J, Scollard DA, Mondal H, Holloway C, Kahn HJ, Reilly RM. Imaging of HER2/neu-positive BT-474 human breast cancer xenografts in athymic mice using ^{111}In-trastuzumab (Herceptin) Fab fragments. Nucl Med Biol 2005; 32:51-8; PMID:15691661; http://dx.doi.org/10.1016/j.nucmedbio.2004.08.003
45. Stabin MG, Sparks RB, Crowe E. OLINDA/EXM: the second-generation personal computer software for internal dose assessment in nuclear medicine. J Nucl Med 2005; 46:1023-7; PMID:15937315
46. Soret M, Bacharach SL, Buvat I. Partial-volume effect in PET tumor imaging. J Nucl Med 2007; 48:932-45. PMID:17504879; http://dx.doi.org/10.2967/jnumed.106.035774
47. Costantini DL, McLarty K, Lee H, Done SJ, Vallis KA, Reilly RM. Antitumor effects and normal-tissue toxicity of ^{111}In-nuclear localization sequence-trastuzumab in athymic mice bearing HER-positive human breast cancer xenografts. J Nucl Med 2010; 51:1084-91; PMID:20554744; http://dx.doi.org/10.2967/jnumed.109.072389.